ASSESSING RE-EMERGING ANGIOGENIC PROPERTIES ASSOCIATED WITH

ARTERIOVENOUS MALFORMATION RELATED TO HHT

AN HONORS THESIS

SUBMITTED ON THE FOURTH DAY OF MAY, 2021

TO THE DEPARTMENT OF CELL AND MOLECULAR BIOLOGY

IN PARTIAL FULFILLMENT OF THE REQUIREMENTS
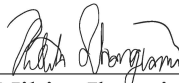
OF THE HONORS PROGRAM

OF NEWCOMB-TULANE COLLEGE

TULANE UNIVERSITY

FOR THE DEGREE OF BACHELOR OF SCIENCE

WITH HONORS IN CELL AND MOLECULAR BIOLOGY

BY

_____
Nikita Jhangiani

APPROVED:

_____
Stryder Meadows, Ph.D.
Director of Thesis

_____
Shusheng Wang, Ph.D.
Second Reader

_____
Adam McKeown, Ph.D.
Third Reader

Nikita Jhangiani. Assessing Re-Emerging Angiogenic Properties Associated with Arteriovenous Malformation Related to HHT.

(Professor Stryder Meadows, Cell and Molecular Biology)

My Honors Thesis is focused on the human genetic disorder called Hereditary Hemorrhagic Telangiectasia (HHT). This disease affects the vascular system and is present in approximately 1 in 5000 people. The most severe symptom in these patients is the formation of arteriovenous malformations (AVMs). AVMs result from arteries and veins improperly connecting. The goal of this project is to better understand the molecular and genetic causes of AVMs, which are currently unknown. The Meadows lab has developed a mouse model that forms AVMs in the retina when knocking out the gene Smad4, which is known to be a transcriptional regulator in the TGFβ pathway. By knocking out the transcriptional regulator Smad4, the Meadows lab has identified potential downstream molecules responsible for the development of AVMs. Three of these genes, Angiopoietin 2 (Ang2), Apelin (Apln), and Endothelial Cell Specific Molecule 1 (Esm1), are hypothesized to be inhibited by Smad4, since when Smad4 is knocked out, Ang2, Apln, and Esm1 are being found to be overexpressed. Interestingly, these genes are implicated in the active process of angiogenesis, which is thought to be upregulated and responsible for AVM formation. Using this mouse model and molecular biology lab techniques, I have measured the effect of the loss of Smad4 as it results in the overproduction of Ang2, Apln, and ESM1 at the transcriptional level and tested whether Smad4 regulates the transcription of these genes. These findings confirm that Smad4 is directly involved in the repression of these genes, further indicating their repression is important to inhibiting AVM development.

Acknowledgements

I would like to thank Xingyan Zhou, the Ph.D. student in Dr. Meadows' lab who has worked very closely with me for the last three years and has trained me to be proficient in all of the molecular laboratory techniques I needed to complete my thesis. Her endless support, guidance, and friendship has made me the student I am today. I would also like to thank former and current members of the Meadows Lab; Dawn Westhoff, Nehal Patel, Angela Crist, Avery Blanks, and Dr. Stryder Meadows himself. My Cellular and Molecular Biology professors such as Dr. Frank Jones, Dr. Meenakshi Vijayaraghavan, and Dr. Elizabeth Abboud have also supported me greatly and taught me the information and skills I needed to complete this thesis effectively. Lastly, I'd like to thank my parents, Lalit and Juthica Jhangiani, my sister, Geeta Jhangiani, and my friends for supporting me as I undertook this endeavor and in everything I do.

TABLE OF CONTENTS

LIST OF FIGURES

Introduction

An Overview of Hereditary Hemorrhagic Telangiectasia

Hereditary Hemorrhagic Telangiectasia (HHT) is a familial, autosomal dominant disorder that affects approximately 1 in 5-8000 people worldwide (Kjeldsen, 1999). Affected individuals present with nasal and gastrointestinal bleeding, which is associated with anemia. Gastrointestinal bleeding has been shown to increase in severity in age, however with nosebleeds, that trend is less clear (Plauchu, 1989). Individuals affected by HHT also present with telangiectasia on the lips and fingertips, which is the presence of visible dilated blood vessels.
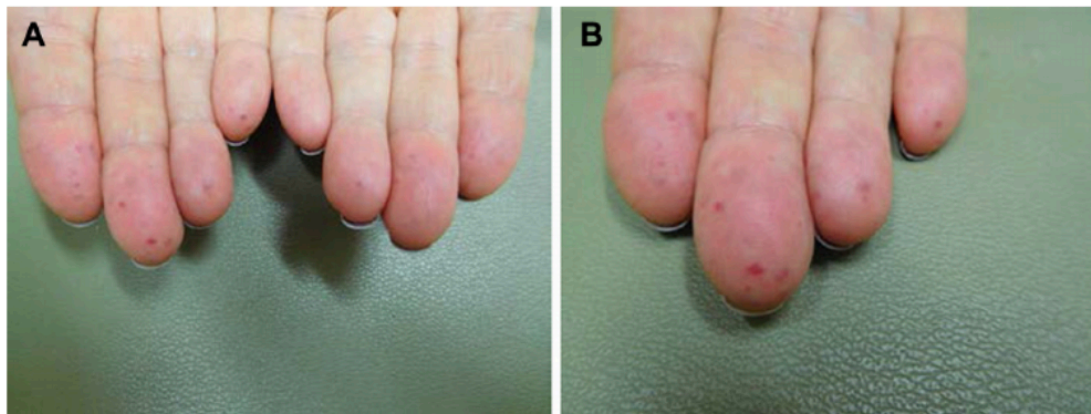
Figure 1 Distal (A) and closer (B) views of prominent telangiectases on the fingertips of a 74-year-old woman with hereditary hemorrhagic telangiectasia (HHT) (Bari, 2017).

Additionally, HHT patients have larger arteriovenous malformations (AVMs) in the pulmonary, hepatic, cerebral, pancreatic, spinal and other circulations (Guttmacher, 1995). Cerebral and pulmonary AVM development is typically completed by the end of puberty, however they typically enlarge and burst later in age. Other symptoms that have recently been identified and tied to HHT include pulmonary arterial hypertension,

juvenile polyposis, high output cardiac failure secondary to hepatic AVMs, and immune dysfunction (Shovlin, 2010).
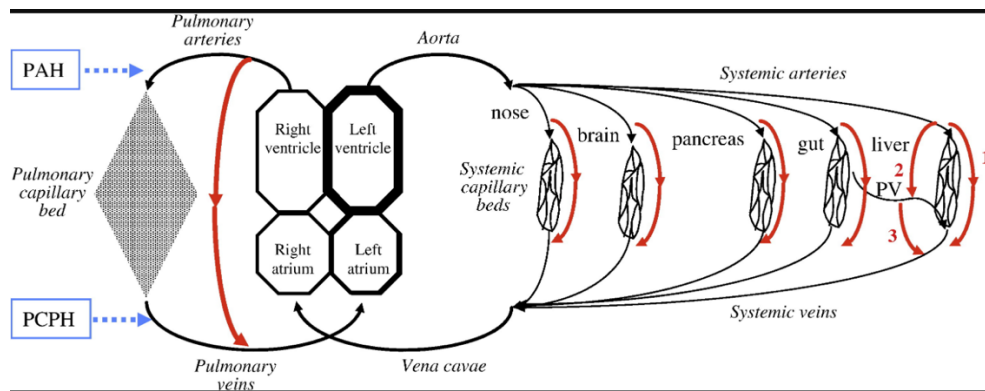
Figure 2 Schematic of systemic and pulmonary circulations indicating vascular beds commonly affected by HHT. Red arrows show AVMs. PV = portal vein; PAH = site of pulmonary arterial hypertension; PCPH = site of post capillary pulmonary hypertension (Shovlin, 2010).

In this thesis, the symptom of HHT that is of greatest focus is the formation of AVMs. AVMs are direct connections between arteries and veins in the absence of a capillary network and are one of the deadlier symptoms of HHT (Lawton, 2015). Larger AVMs, which are typical of HHT patients, are postulated to arise from the constant vascular remodeling of smaller lesions (Braverman, 1990). Normally, when veins are moved to be in arterial settings, the vessels adapt to support higher arterial pressure by increasing their wall thickness. This is essential to maintain an optimal wall thickness/lumen radius ratio to minimize vessel wall stress (Owens, 2010). In patients with HHT, this adaptation does not take place. The formation of AVMs in these patients is detrimental because instead of increasing the thickness of the vessel walls, the vessels dilate, and the walls thin, which does not support the arterial pressure, and can cause the AVMs to burst (Owens, 2010). When AVMs burst, depending on their locations, they can cause stroke and even death.
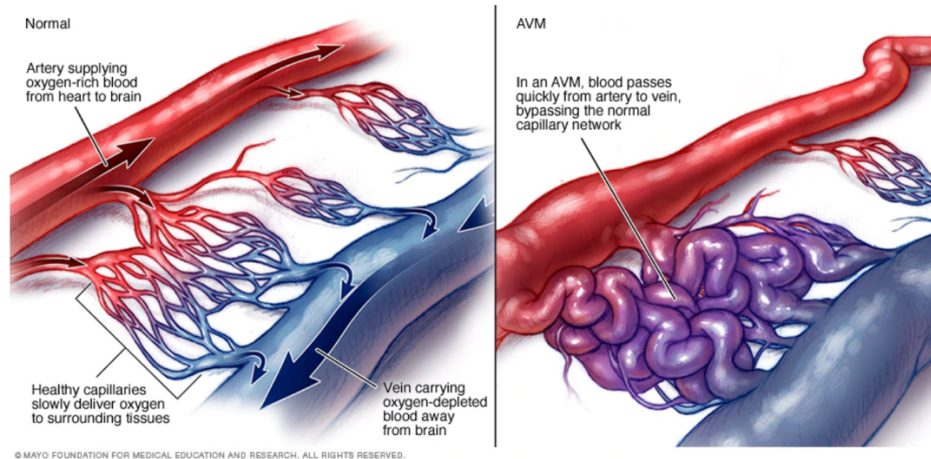
Figure 3 Normal arterial-venous connection vs. an arteriovenous malformation (Mayo Clinic, 2015).

When studying HHT, researchers have identified five known subtypes, each characterized by their associated autosomal dominant genetic mutations. Most studies of HHT have been focused on HHT1 and HHT2. HHT1 presents with mutations in the Endoglin (ENG) gene and is the most prevalent form of HHT (McAllister, 1994). HHT2 is the second most common form of HHT and is characterized by mutations in ACVRL1 encoding activin receptor-like kinase (ALK1) (Johnson, 1996). Mutations in ENG and ALK1 make up of 90% of the mutations observed in HHT. In one to two percent of cases of HHT, it has been identified that patients have mutations in Mothers against decapentaplegic homolog 4 (SMAD4) (Shovlin, 2010). The last two subtypes which can cause HHT phenotypes have been localized to mutations on chromosome 5q and chromosome 7p (Bayrak-Toydemir, 2006), but the genes have not been identified.

HHT Types	GEN	Chromosomal Locus
HHT 1	Endoglin or ENG	9q34.1
HHT 2	Activin Receptor-like Kinase 1, (ACVRL1/ALK 1)	12q11 - q14
HHT 3	-	5q31.3 - q32
HHT 4	-	7p14
HHT + juvenile polyposis coli	MADH4 or SMAD4	18q21.1
HHT 2 + primary pulmonary hypertension	BMPRII	2q33

Figure 4 Genetics of hereditary hemorrhagic telangiectasia (Gomez, 2015).

Since HHT1 and HHT2 are the most commonly known forms of the disorder, most research on HHT has been focused on their molecular and genetic causes that give rise to HHT phenotypes in human patients. In HHT1 and 2, mutations occur throughout the genetic sequence of ENG and ALK1 respectively, with no distinct loci or focal points for common mutations in the sequence. These mutations range from single base pair changes to major deletions, but all result in the formation of a nonfunctional protein product, which leads to haploinsufficiency conditions in both subtypes of the disorder (Botella, 2015). Patients with HHT1 present with pulmonary and cerebral AVMs, as well as microscopic intrapulmonary shunting, whereas patients with HHT2 have a higher prevalence of hepatic AVMs and a lesser occurrence of pulmonary AVMs. Due to the high presence of hepatic AVMs, patients with HHT2 also have a higher risk for pulmonary arterial hypertension (Shovlin, 2010).

Smad4 Model of HHT

Little is known about the 1-2% of patients with HHT that have mutations in SMAD4. Some studies have shown that SMAD4 mutations in HHT tend to be localized in the part of the gene encoding the MH2 domain, which would hinder the capacity of SMAD4 to bind to other R-SMADs, but other studies have shown that HHT-causing mutations can also occur in other parts of SMAD4 (Gallione, 2010). Phenotypically, HHT patients who have mutations in SMAD4 have the highest incidence of pulmonary arteriovenous malformations, which is the most severe symptom in this disorder (Gallione, 2004). Additionally, juvenile polyposis syndrome, which is a disorder characterized by precancerous epithelial polyps in the large intestine typically due to a mutation in the BMP type I A receptor (BMPR1A), is also seen to occur in patients with SMAD4 mutations.
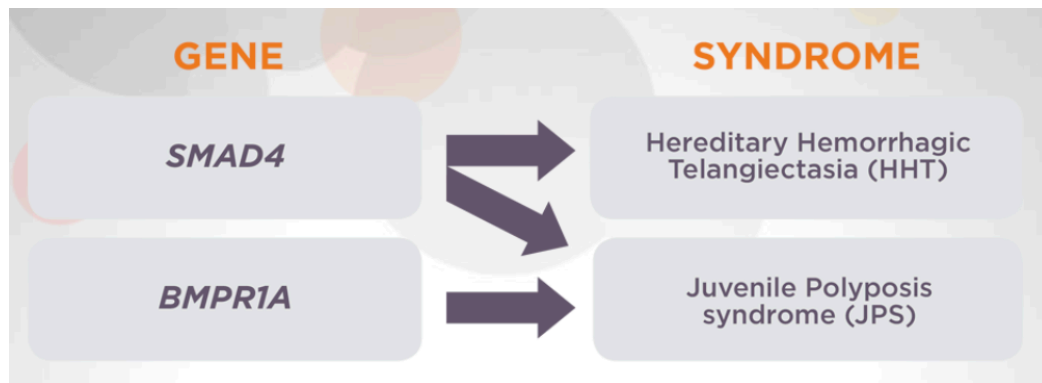
Figure 5 A graphic showing a Smad4 mutation can lead to HHT and JPS (Project DNA, 2020).

ENG, ALK1, and SMAD4 are genes that encode proteins that mediate signaling in the transforming growth factor (TGF)-β superfamily, which has many effects on cellular proliferation, differentiation, morphogenesis, tissue homeostasis and regeneration

(Massagué, 2012). Typically, TGF-β signaling has an inhibitory effect on growth in endothelial cells, however when there are mutations in the pathway, the cellular functions that the signaling pathway usually inhibits are free to progress. Of interest in HHT, TGF-β signaling in endothelial cells is able to modulate angiogenesis and vascular remodeling (Blanco, 2005). There are two ligand subfamilies: the TGFβ-activin-Nodal and the bone morphogenetic protein (BMP) subfamily, and both bind to a heteromeric complex of type I and type II transmembrane serine/threonine kinase receptors in the plasma membrane. In the TGF-β-activin-nodal branch, the type II receptor binds to the ligands with high affinity, but in the BMP branch, the receptors have low affinity for ligand, and this is only enhanced by membrane colocalization (Groppe, 2008).
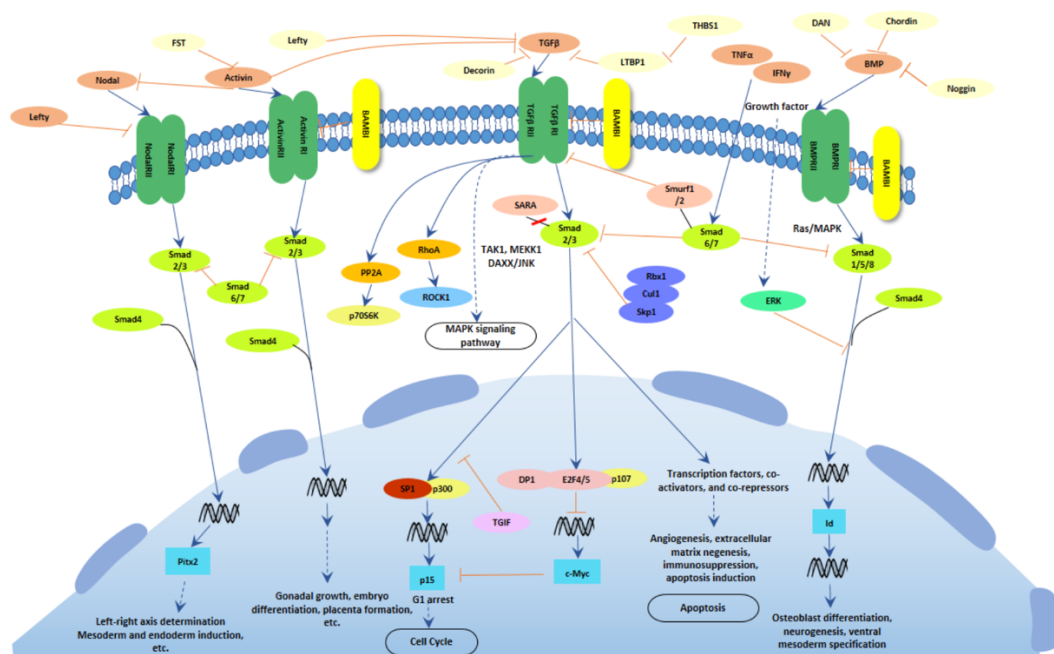
Figure 6 TGF-β Superfamily Signaling depicting downstream effects (Cusabio, 2020).

When a ligand (TGF-βs, BMPs, activins, nodals, growth/differentiation factors, and inhibins) binds to a heteromeric complex of receptor serine/threonine kinases (types I and II), it induces transphosphorylation in the type I receptor by the type II receptor kinases. Then, the now activated type I receptors phosphorylate selected Smads, and these receptor-activated Smads (R-SMADS). In the TGF-β-activin-nodal receptor subfamily, Smad2 and Smad3 are activated, and in the BMP subfamily, Smad1, Smad5, and Smad8 are activated. The R-Smads are then released from the receptor complex and form a heterotrimeric complex of two R-Smads and a common Smad4 (Masuyama, 1999). Together, the activated Smad complex translocates into the nucleus and regulates the transcription of target genes by recruiting coactivators (Derynck, 2003). Cross talk can occur with other signal transduction cascades which can have a downstream effect in the TGF-β signaling pathway.
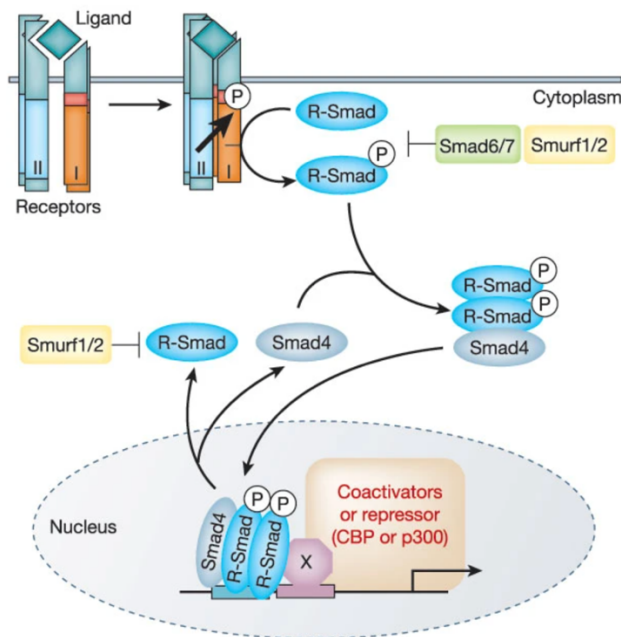
Figure 7 General mechanism of TGF-β receptor and Smad activation (Derynck, 2003).

As previously mentioned, the R-Smads and Smad4 have a MH2 domain, which is how they can bind to each other, the receptor, and interact with inhibitory Smads 6 and 7 to be targeted for degradation. Additionally, R-Smads and Smad4 contain a conserved MH1 domain which allows them to interact with transcription factors and bind to DNA.
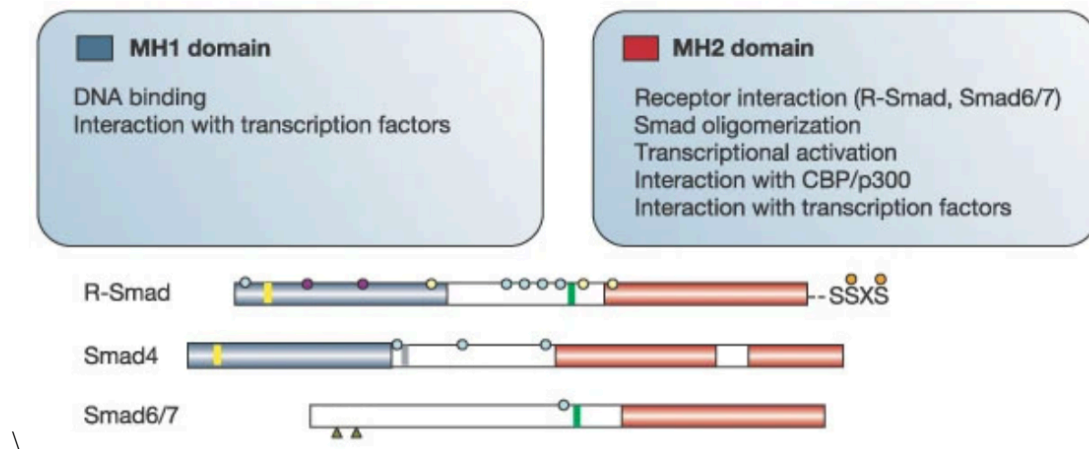
Figure 8 Structural organization and role of the domains of Smads (Derynck, 2003).

Endoglin (ENG) is an endothelial cell-specific accessory protein, or co-receptor, for many receptor complexes in the TGF-β superfamily, and its interaction with ALK-1 is of most interest within the context of HHT (Barbara, 1997). Expression of endoglin counteracts the TGF-β-induced growth inhibition in endothelial cells (Li et al., 2000). ALK-1 is an endothelial-specific type I receptor that belongs to the BMP branch of type I receptors (Upton, 2009). ALK-1 is able to associate with two type II receptors, BMPR2 and TβRII. TβRII can associate with different TGF-β type I receptors in endothelial cells (ALK-5 and ALK-1), and these associations are modulated by endoglin. Active ALK-1 leads to increased endothelial cell proliferation and angiogenesis, whereas active ALK-5 decreases cell proliferation and angiogenesis. ALK-1 and ALK-5 activate different Smads, which then activate Smad4. Haploinsufficiency or loss of ALK1 or ENG results

in the HHT-associated phenotypes, as the remaining wild type allele is unable to contribute sufficient protein for normal function (Shovlin, 2010).
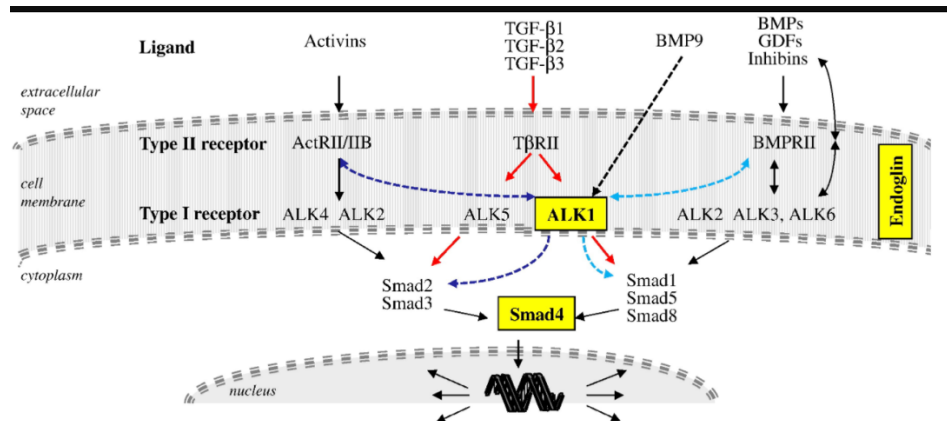
Figure 9 TGF-β superfamily signaling in endothelial cells. Yellow boxes indicate proteins encoded by HHT genes (Shovlin, 2010).

Animal studies have been focused on creating mouse models with ENG and ACVRL1 mutations. Null mice showed embryonic homozygous lethality, but heterozygous mice expressed HHT-like phenotypes. Inducible homozygous loss of ALK1 and ENG in vivo has showed AVM formation in previous HHT animal studies, but they have not shown the *in vivo* role of Smad4 in vasculature (Crist et. al, 2018). Chapter 2 will discuss previous research done in the Meadows Lab creating a mouse model to better understand how mutations in Smad4 lead to AVM formation. The creation of Smad4 HHT mouse models was deemed essential by the Meadows Lab to identify the downstream regulators of HHT since Smad4 is a central transcription factor in the TGF-β pathway, and since the downstream genes and proteins in AVM formation are poorly understood.

The Effects of Vascular Deficiency of Smad4

Understanding of the previous research done in 2018 by the Meadows lab is imperative in order to articulate the purposes of my current research. The main goal of their research was to identify the effects of a Smad4 deletion in the endothelial cells, as seen in ~4% of patients with HHT. As mentioned previously, a mouse model had not been created until the work of their lab, since homozygous loss of Smad4 is embryonic lethal. Therefore, the Meadows lab set out to create an inducible, Smad4 endothelial-cell specific knockout (Smad4-iECKO) mouse in order to study the vascular development in HHT.

In order to create the Smad4-iECKO mouse, the researchers crossed a Cdh5-Cre^ERT mouse line with a conditional Smad4-floxed mouse line to generate a homozygous mouse line (Crist et.al, 2018). Tamoxifen was administered on postnatal days 1 and 4 in order to activate the Cre-mediated deletion of Smad4 only in the endothelium.
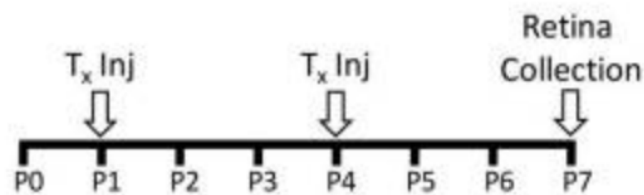
Figure 10 A schematic depicting the tamoxifen injections and retina collections of the control and Smad4-iECKO mice (Crist et.al, 2018).

In order to confirm the deletion of Smad4, qPCR was performed and found to have an 80% reduction in the mRNA transcripts of Smad4 in the Smad4-iECKO models compared to the control (Crist et.al, 2018).
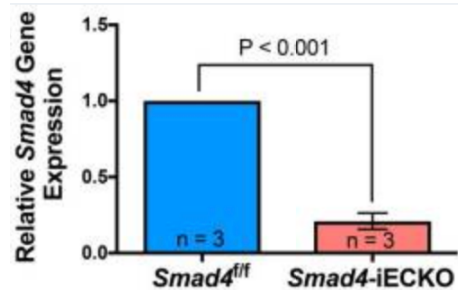
Figure 11 A graph showing the Smad4 mRNA knockdown level (Crist et.al, 2018).

After a successful creation of the Smad4-iECKO model, the effects of the vascular deficiency of Smad4 were studied using isolectin-IB4 -staining of retinas. First, in 82% of the Smad4 mutants, there were AVMs in their retinas, whereas AVMs were absent in the controls (Crist et.al, 2018). These AVMs were similar to those identified in previous research studying Alk-1 and Eng-deficient mice traditionally used to model HHT (Mahmoud, 2010) (Oh, 2000). The formation of AVMs in these Smad4-deficient mice proved the Smad4-iECKO model to be a successful model for HHT, since AVMs are one of the most characteristic phenotypes of the disease.
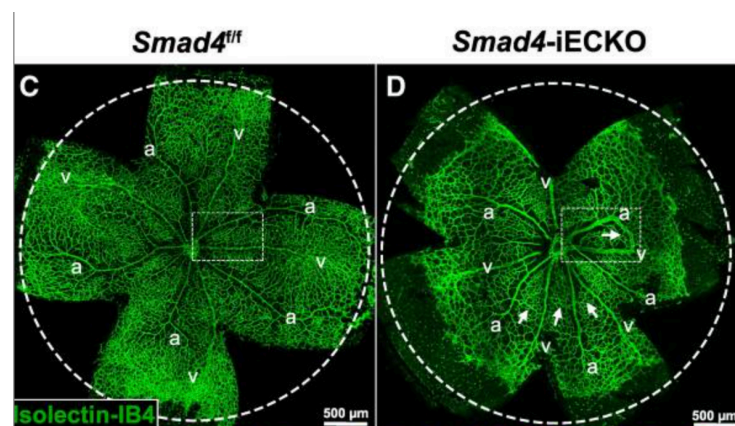
Figure 12 Retinal imaging comparing the control and Smad4-iECKO vasculature development. The arrows in the image on the right point to AVMs. The image on the left has no AVMs (Crist et.al, 2018).

In the retinal imaging, the loss of Smad4 also showed a reduction in vascular outgrowth toward the retinal periphery. Due to this finding, and previous research using Alk1 mutant zebrafish showed that endothelial cells had migratory defects (Rochon, 2016), further investigation of Smad4 and its role on endothelial migration was done in vitro. In a scratch assay using stable mouse endothelial cell lines, Smad4-shRNA cells showed a 60% reduction in the levels of Smad4 transcripts compared to cells with nonsilencing-shRNA, and a lesser capacity to migrate in a scratch assay (Crist et.al, 2018).
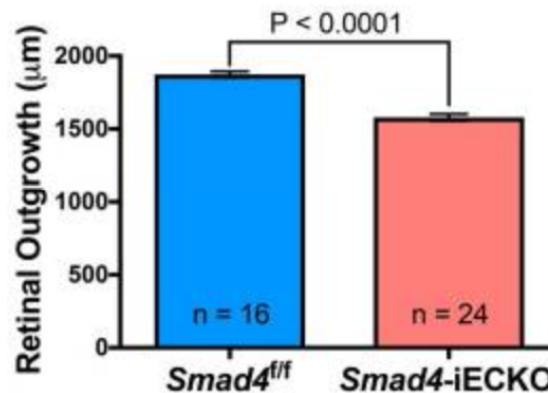
Figure 13 A graph showing the reduction in retinal outgrowth of the Smad4-iECKO retinal vasculature compared to the control (Crist et.al, 2018).

Additionally, the retinal imaging showed an increase in both the diameter of the arteries and the veins due the Smad4 reduction. In order to determine whether this vessel enlargement was due to an increase in endothelial cell proliferation or an increase in endothelial size, further studies were done by the Meadows lab.
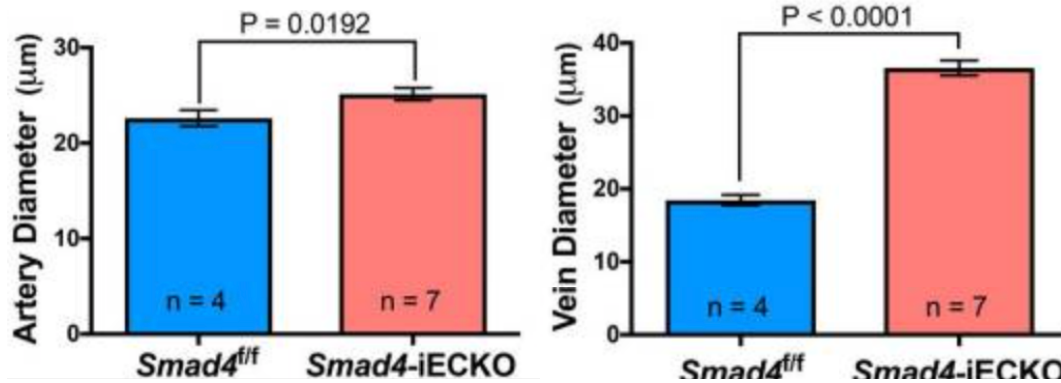
Figure 14 Graphs showing the increase in diameter of both the arteries and veins in the Smad4-iECKO model compared to the control (Crist et.al, 2018).

By quantifying the proliferating endothelial cells in arteries, veins and capillaries of the retinas, it was found that the Smad4 reduction caused an increase in the endothelial cell proliferation, most drastically in the capillaries and veins (Crist et.al, 2018). These increases in proliferation occurred in vascular regions with and without AVMs, which means increased endothelial cell proliferation is not an effect of AVM formation by itself, but due to the reduction in Smad4.
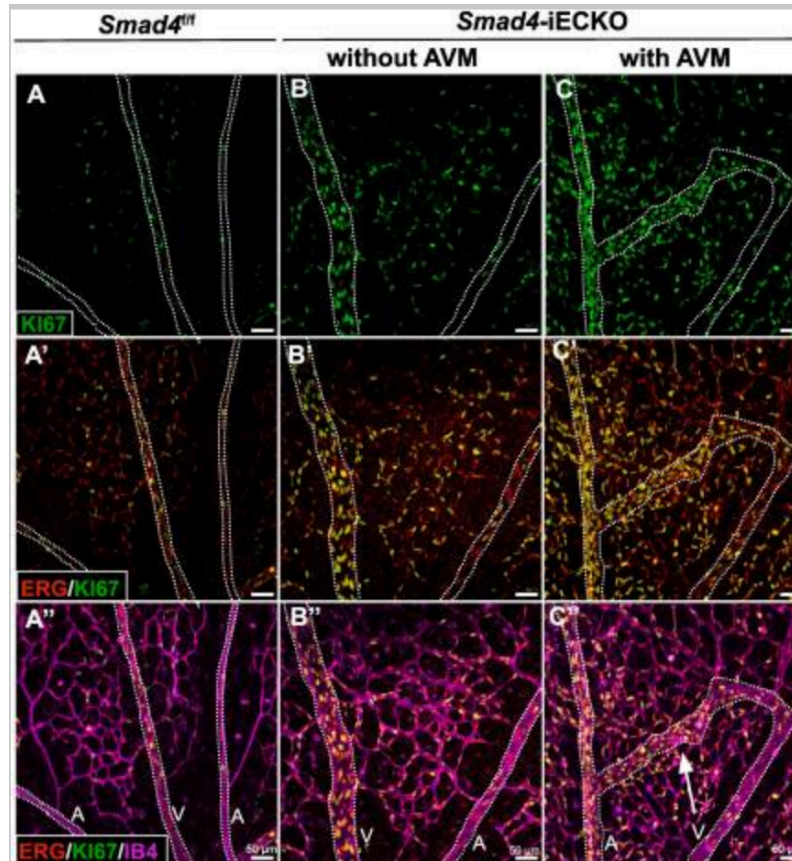
Figure 15 Confocal imaging showing the increased presence of K167 and ERG, which are indicators of endothelial cell proliferation, in the Smad4-iECKO vasculature compared to the control. Additionally, there is an increase in the Smad4-iECKO vessels containing an AVM compared to the vessels without an AVM (Crist et.al, 2018).

Since previous research has shown that the loss of Eng or Smad4 can lead to increased endothelial size (Poduri, 2017), the Meadows lab also investigated if the Smad4-iECKO mice exhibited changes in cell size by measuring the areas in each vessel type. The Smad4 deletion caused the cell area of both the arterial and venous endothelial cells to increase by 34-41% when compared to control vessels (Crist et.al, 2018). They were able to conclude that a combination of increased endothelial cell proliferation and size contributes to the vessel enlargement seen in Smad4 mutants.
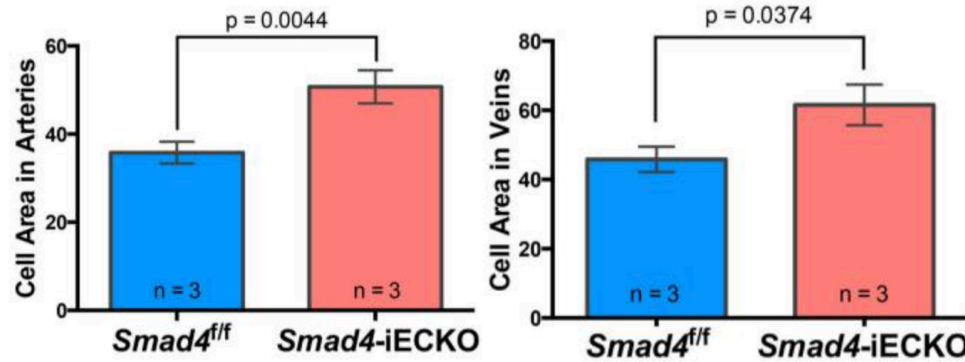
Figure 16 Graphs showing the increased cellular areas in arteries and veins in the Smad4-iECKO models (Crist et.al, 2018).

In previous HHT research, it has been shown that there were changes in the mural cell coverage of retinal blood vessels in Alk1 and Eng models of HHT with the presence of vascular smooth muscle cells (Mahmoud, 2010). In the Smad4-iECKO mice, the Meadows lab also observed strong, ectopic expression of alpha-smooth muscle actin (aSMA) protein, which is present in muscle cells, around the AVMs and veins, compared to control retinas, which only exhibit (aSMA) on arteries (Crist et.al, 2018). This is indicative of the changes in the mural cell coverage.
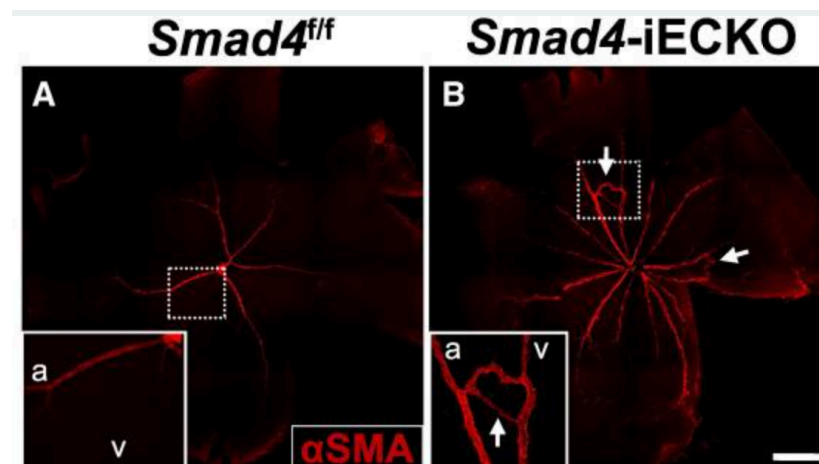
Figure 17 Retinal imaging showing the increased presence of aSMA in the Smad4-iECKO retinas compared to the control (Crist et.al, 2018).

Lastly, previous research has shown that AVMs are associated with a reduction in pericyte coverage (Baeyens, 2016). To test whether this relationship exists in *Smad4-*

iECKO retinas, the Meadows lab investigated pericyte coverage using an anti-neuron-glial antigen 2 (NG2) antibody. They found that, compared to controls, *Smad4* mutant retinas exhibited a reduction in NG2 protein accumulation in the retinal vasculature, which signifies the reduction in pericyte coverage (Crist et.al, 2018).
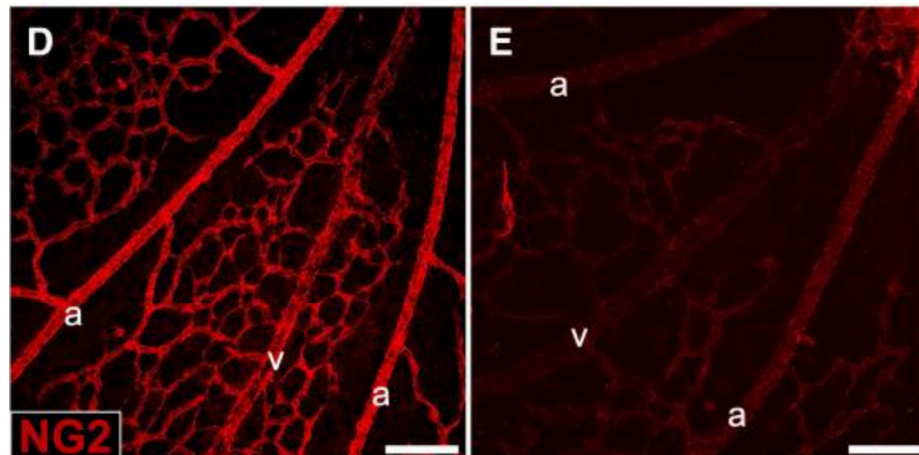
Figure 18 Retinal imaging showing the decrease in presence of NG2 in the Smad4-iECKO retina (right) compared to the control (left) (Crist et.al, 2018).

These findings (the formation of AVMs, the increase in endothelial cell proliferation and size, the changes in mural cell coverage, and the reduction in pericyte coverage) show that the loss of Smad4 contributes to various angiogenic phenotypes seen in HHT. Further investigation as to how Smad4 has these effects is currently being investigated by the Meadows lab and will be described in the next section.

Smad4 Is a Direct Transcriptional Repressor of Angpt-2

Further studies done by the Meadows Lab have been conducted to identify how the loss of Smad4 directly contributes to angiogenesis and the formation of AVMs. Comparing RNA sequencing studies of Smad4-iECKO-isolated retinal endothelial cells (mutant) and Smad4 f/f isolated retinal endothelial cells (control) revealed 1905 differentially expressed genes (Crist et.al, 2019).
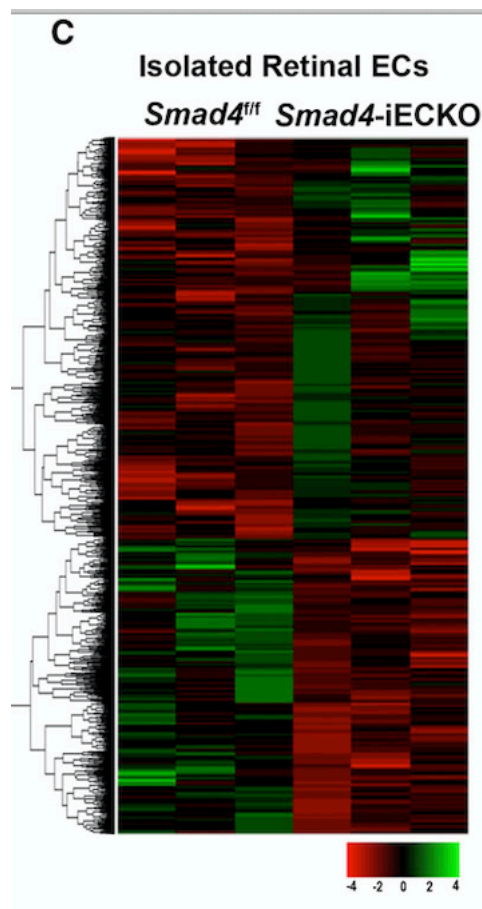
Figure 19 RNA sequencing studies showing differentially expressed genes between Smad4 f/f and Smad4-iECKO isolated retinal endothelial cells (Crist et.al, 2019).

Additionally, since BMP9/10 ligands bind to ACVRL1 and ENG receptors, which are upstream from Smad4 in the TGFβ pathway (Saito, 2017), the Meadows Lab conducted ChIP-Seq experiments on BMP9/10-stimulated and unstimulated mouse

endothelial cells. They found Smad4 binding sites in 613 genes in the unstimulated

conditions and 1806 genes in the stimulated condition, 490 of which were shared between

the two (Crist, 2019).
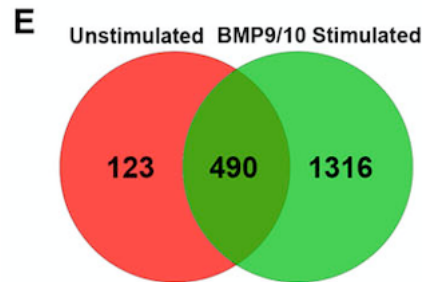
Figure 20 490 shared genes between the BMP9/10 unstimulated vs. stimulated
conditions (Crist et.al, 2019).

Combining the RNA and ChIP sequencing studies above identified 212

overlapping direct, downstream effectors of Smad4 which are critical in HHT-related

AVM formation.
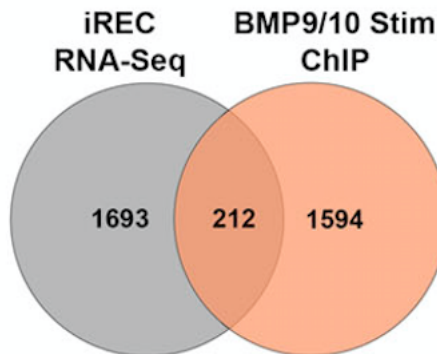
Figure 21 212 possible effectors downstream of Smad4 were identified through RNA
and ChIP sequencing (Crist et.al, 2019).

They found two critical genes in this data set, which are important in the

angiopoietin-Tek signaling pathway: the cell surface receptor, TEK and its antagonistic

ligand, ANGPT2.
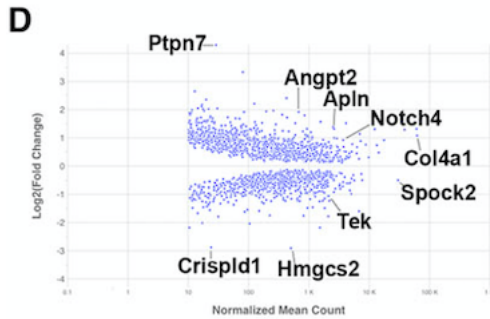
Figure 22 RNA sequencing study showing the overexpression of Angiopoeitin-2 (Angpt2) and Apelin (Apln), and downregulation of Tyrosine Receptor Tyrosine Kinase (Tek) (Crist, 2019).

This pathway is known to be important in vascular development, and has been found to have important functions during embryonic vessel assembly and maturation (Augustin, 2009). Tek receptors are normally found in endothelial cells, and activation of these receptors promotes endothelial cell survival and vascular assembly, stability, and maturation. This complements VEGF signaling which initiates events in angiogenesis such as endothelial cell sprouting (Thurston, 2012). In the Angiopoietin-Tek pathway, Angiopoeitin-1 is responsible for activating Tek, and Angiopoeitin-2 is antagonistic, repressing Tek's effects (Thurston, 2012).
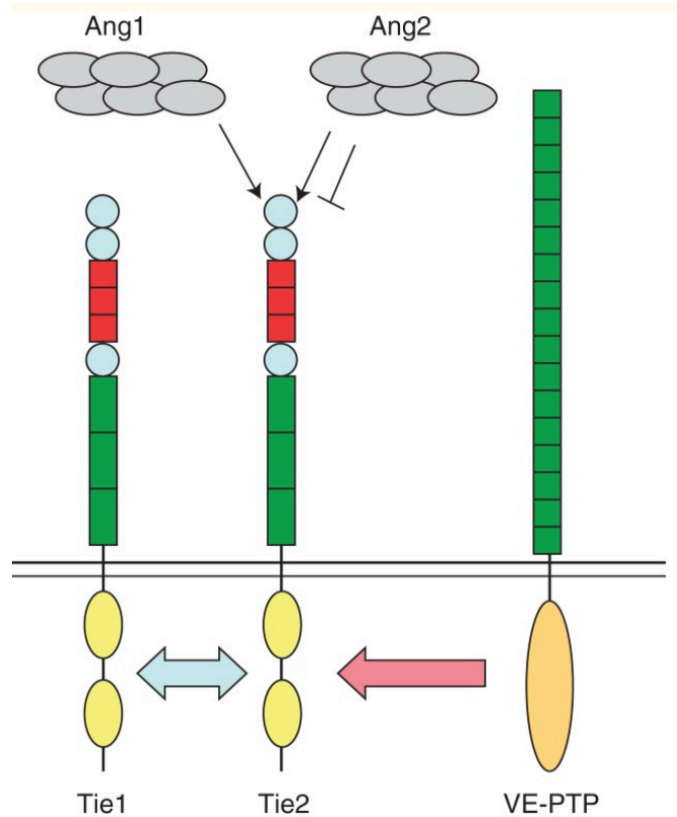
Figure 23 A diagram articulating the Angiopoeitin-Tie2(Tek) signalling pathway (Thurston, 2012).

In the Meadows Lab, they found that the expression levels of Tek receptor tyrosine kinase (Tek), were decreased and Angiopoietin-2 (Angpt2) were increased in the Smad4-iECKO mice, which led to a net reduction in TEK signaling (see **Figure 21**).

Additionally, in situ hybridization on P7 retinas showed that when Smad4 is lost, Angpt2 becomes highly upregulated in the growing vascular front, but is absent from the AVMs, and Tek is diminished in the arteries, veins, and capillaries, but accumulates at the AVMs (Crist et.al, 2019). Normally, Angpt2 is expressed at very low levels in the growing vascular front and Tek is expressed throughout the vasculature.

In order to assess if Smad4 directly regulates the transcription of Angpt2 in the endothelium, the Meadows Lab utilized ChIP-qPCR to ascertain if there were Smad4 binding sites on the Angpt2 and Tek genes. They found one binding site in the first intron of the Tek gene, but it was not evolutionarily conserved. However, they found 3 binding sites upstream of the Angpt2 gene, which were evolutionarily conserved.
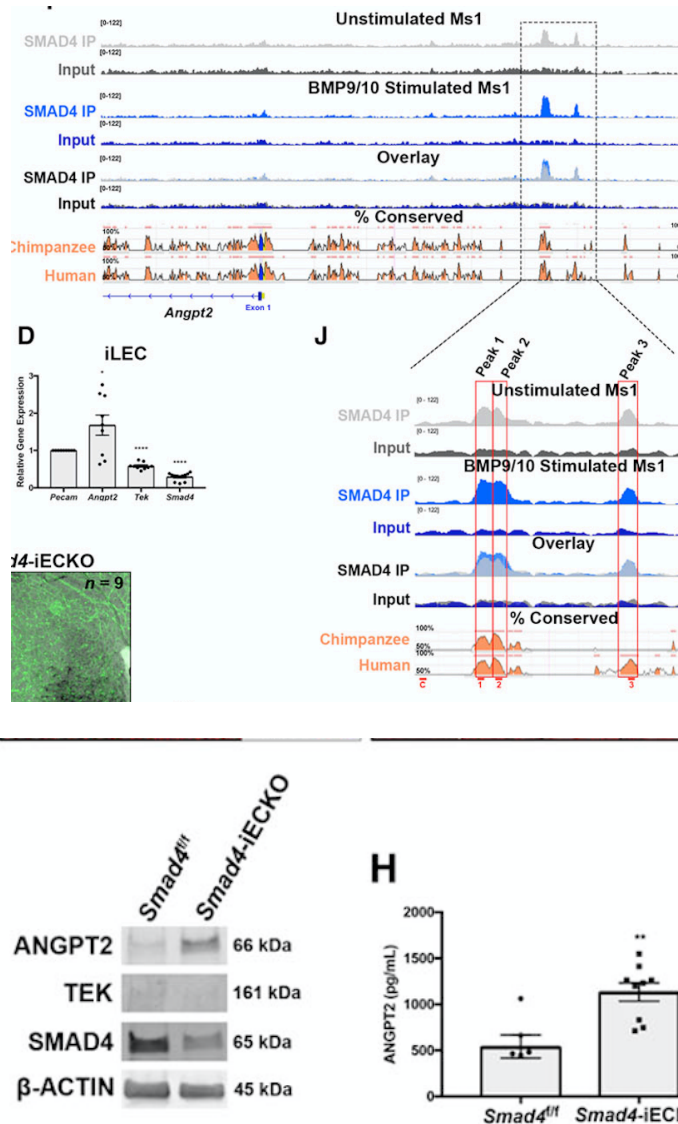
Figure 24 Diagrams showing the ChIP-qPCR, Western Blot, and qPCR results that established Smad4 binding on the Angiopoietin-2 gene, as well as absence of Smad4 leading to overexpression of Ang-2 at both the protein and RNA level (Crist et.al, 2019).

Additionally, ChIP-qPCR studies confirmed Smad4 binding in BMP9/10 stimulated and unstimulated conditions of Angpt2, and Luciferase assays confirmed repressive transcriptional activity of Smad4 (Crist, 2019).
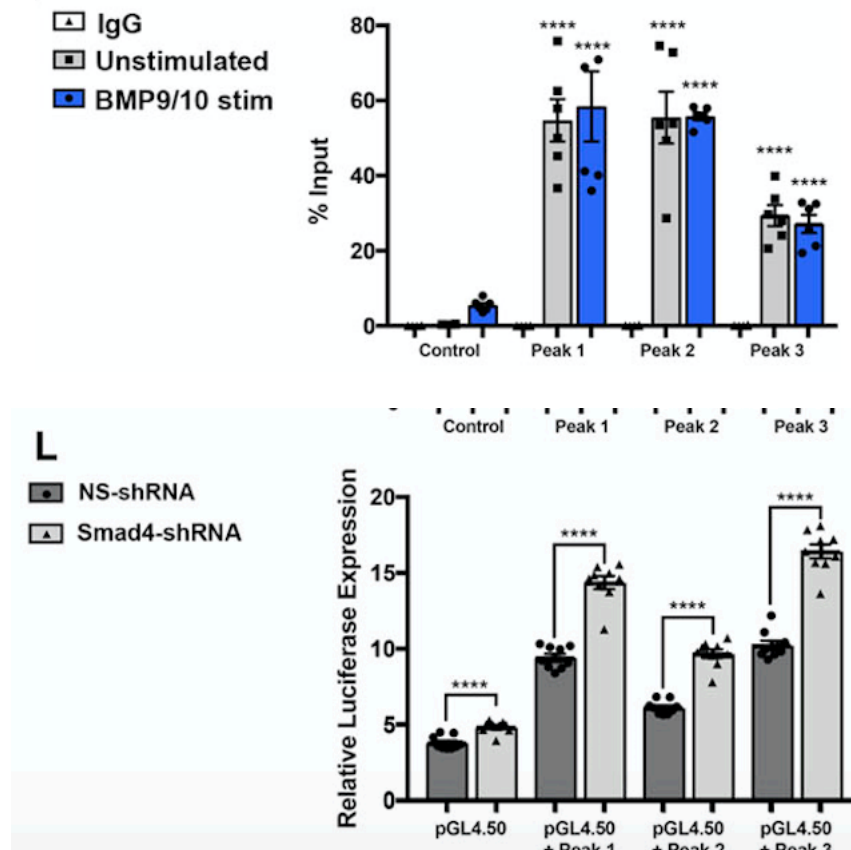
Figure 25 Diagrams articulating the ChIP-qPCR and Luciferase Assay results at all three peaks of Smad4 binding to Angiopoeitin-2 (Crist et.al, 2019).

Therefore, the work done by graduate students in the Meadows lab established a direct mechanistic link between the TGF- β pathway (Smad4) and the angiopoietin-Tek signaling pathway whereby Smad4 is directly responsible for Angpt2 expression in endothelial cells, and acts as a direct transcriptional repressor (Crist, 2019). In order to further test this, the Meadows lab also tested the effects of inhibition of Angpt2 in Smad4-iECKO mice. They found that the inhibition of Angpt2 can prevent AVM

formation, prevent changes in endothelial cell size and shape caused by the loss of
Smad4, can rescue AVMs that were already formed, as well as other cell morphological
effects causes by the loss of Smad4 (Crist, 2019).

Still, further direct effects of Smad4 are unknown. Unpublished in the article, the
Meadows lab also found Apelin (Apln) and Endothelial Specific Molecule-1 (Esm1) to
be overexpressed in the combined data set between RNA and ChIP sequencing (see
Figure 21).

Apln is the ligand for the APJ receptor, which is a G-protein-coupled receptor.
When this receptor is activated, it promotes the formation of new blood vessels and
activates cell transduction cascades such as ERKs and AKT (Kasai, 2004).
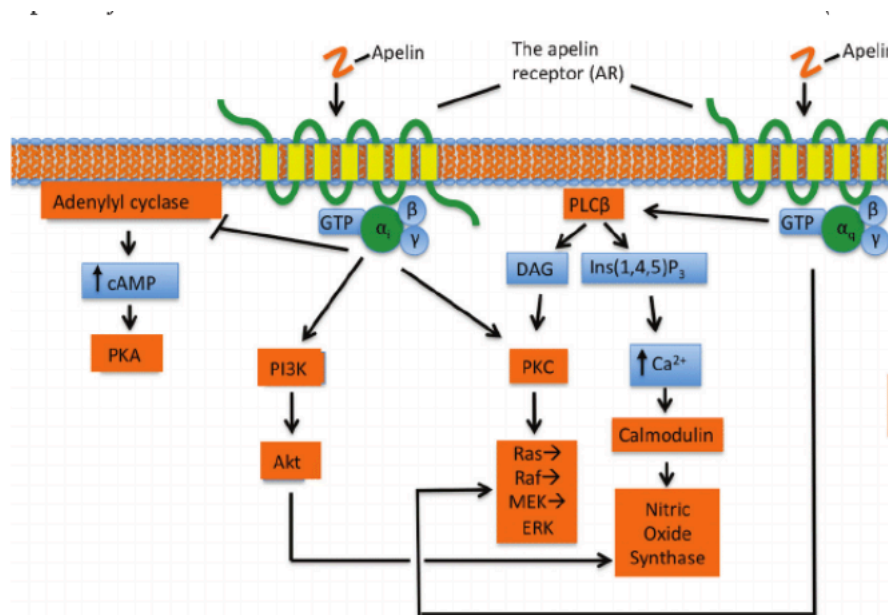
Figure 26 A diagram showing Apelin's signaling pathway, highlighting the
downstream effects it has on AKT and ERK, which are signals that induce blood vessel
formation (Chapman, 2014).

Esm1 is a known biomarker of tip cells during neoangiogenesis. Esm1 expression
is shown to increase in the presence of pro-angiogenic factors such as vascular

endothelial cell growth factor (VEGF) and fibroblast growth factor-2 (FGF-2) (Bechard, 2000).

In short, the expression of Apelin and Endothelial Specific Molecule-1 signals that angiogenesis, or the formation of new blood vessels, is taking place. Overexpression of these genes, as well as Angiopoietin 2, in the Smad4-iECKO HHT model has led to the hypothesis that Smad4 is a transcriptional repressor of all three genes *in vivo*. Therefore, it is hypothesized that it is through this mechanism that mutated Smad4 induces angiogenesis and leads to the formation of AVMs.

Methods

Western Blot

For Western blots, protein was collected using radioimmunoprecipitation assay buffer (Life Technologies 89900), protease inhibitor (Thermo 1860932), and phosphatase inhibitor (Sigma 04906837001), and quantified using Qubit protein assay kit (Thermo Q33211). Sodium dodecyl sulfate polyacrylamide gel electrophoresis was run using 25 to 50 μg of protein mixed 1:1 with lamelli buffer (BioRad 161–0737) and heated to 90°C for 15 minutes and loaded onto a Mini-PROTEAN TGX gel (BioRad 456–8094). After gel electrophoresis, samples were transferred to TransBlot Turbo Transfer Pack 0.2 μm polyvinylidene fluoride membrane (BioRad 1704156) using TransBlot Turbo (BioRad). Membrane was blocked using 5% bovine serum albumin blocking solution for 30 minutes, then primary antibodies were added at a 1:1000 concentration overnight at 4°C. The primary antibodies used were as follows: Anti-βACTIN (Cell Signaling 3700), Anti-Phospho Smad 1/5/9 (ab80255), Anti-SMAD4 (Abcam ab40759), and Anti-GAPDH (Sigma Aldrich PLA0302). After washing, appropriate LICOR IRDye 800CW or 680RD secondary antibodies were used at 1:5000 and incubated at room temperature for 1 hour. Membranes were imaged using Odyssey (LICOR) and iStudio Lite was used for Western quantification.

qPCR and Analysis

All quantitative real-time PCR (qPCR) experiments were performed using RNA isolated with a GeneJET RNA Purification Kit (Thermo K0732) and quantified using a Nanodrop (Thermo). For each sample, 500–1000 ng of RNA was used for cDNA

synthesis using a iScript cDNA Synthesis Kit (Bio-Rad). qPCRs were run using SYBR green mastermix (Thermo K0221) on a Bio-Rad CFX96 Touch Real-Time PCR Detection machine. Analysis was performed using the double delta Ct method, and statistics were generated using GraphPad Prism. For all qPCR experiments, three independent biological replicates were used, and three technical replicates were performed per sample. Primers were verified for specificity and efficiency.

In Vitro Cell Culture

Cells were allowed to grow in DMEM high glucose media. For short hairpin RNA (shRNA) qPCR experiments, MS1 nonsilencing-shRNA and MS1 Smad4KD-shRNA were seeded into two separate six-well plates at a seeding density of 0.3x10^6 cells/well. These cell lines had already been transfected with their respective shRNA vectors and the addition of puromycin selected for the MS1 cells in which the transfection was successful. For stimulation experiments, the plates were place in serum-free DMEM media the night before. The day of collection, 3 wells of each plate were stimulated with BMP 9/10, 4 hours before RNA or protein collection. For short interfering (siRNA) transfection qPCR experiments, MS1 cells were seeded into a six-well plate at a seeding density of 0.1x10^6 cells/well. After 24 hours, transfection took place using the Lipofectamine 3000 Reagent Protocol with control and/or Smad4 SMARTPOOL siRNA vectors. For stimulation experiments, the cells were placed in serum-free DMEM media the evening before. The next morning, the BMP 9/10 stimulated samples were stimulated 1-2 hours before RNA or protein collection took place.

Dual Luciferase Reporter Assay

In order to perform this assay, first MS1 cells were seeded into a six-well plate at a seeding density of 0.3x10^6 cells/well. After 24 hours, 3 wells were transfected with pGL 4.20 vector and 3 were transfected with pGL 4.50 vector using the Lipofectamine 3000+P3000 protocol. The next day, I collected the samples using the Dual Luciferase Reporter Assay protocol (Promega E1910, E1960 AND E1980) for a six-well plate. When placed in the luminometer, the sample signal was too low. Another iteration of this protocol included the same set up with the same vectors, but instead of transfecting with 5 µg of vector DNA, I transfected with 10µg in order to read a signal. Still, the same error showed on the luminometer. Next, I tried transfecting with a known working positive control (pGL 4.50+peak 987nm), with a DNA concentration of 10µg – no signal was shown in both luminometers I tried. Additionally, I tried the same experimental set up with 293T cells, since they are easier to transfect, but the sample signal was still read as too low. I also tried seeding at a lower density (0.1x10^6 cells/well), and letting the cells wait for two days after vector transfection so that the cells have time to assimilate the DNA vectors. I also transfected all of the wells with pGL 4.75 as well as either the pGL 4.50 or pGL 4.50 + peak 987 as previous work had shown that together a signal can be produced in the luminometer. In spite of all these iterations, no signal was able to be read by two different luminometers.

Results

Smad4 shRNA Experiments

Given the *in vivo* findings of previous researchers in the Meadows Lab, confirmation of Smad4 repression of Angpt2, Apelin, and ESM1 *in vitro* would strengthen the hypothesis of Smad4 as a transcriptional repressor of these angiogenic effectors. To knockdown Smad4 *in vitro*, RNA interference in the form of shRNA or siRNA may be used to selectively and specifically knockdown a targeted gene. Since previous researchers in the Meadows Lab had already created Nonsilencing and S4KD shRNA MS1 cell lines, I elected to use those first. I seeded 1x six-well plate with 3 wells of Nonsilencing shRNA MS1 cells and 3 wells of Smad4KD shRNA MS1 cells at a seeding density of 0.3x10^6 cells/well.

Figure 27 A schematic showing the basic Nonsilencing and Smad4KD shRNA experimental design.

Smad4 knockdown level using the shRNA model was confirmed via protein collection and a Western blot.
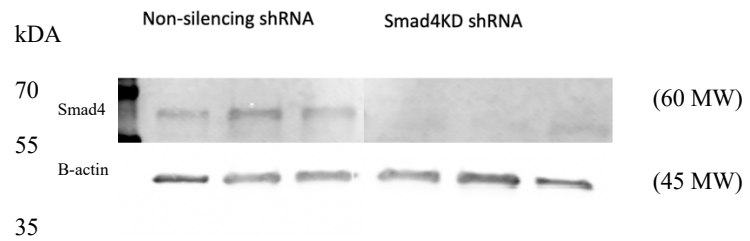
Figure 28 Western Blot showing the absence of Smad4 protein in the shRNA model.

As mentioned previously, since BMP9/10 ligands bind to ACVRL1 and ENG receptors, which are upstream from Smad4 in the TGFβ pathway, *in vitro* BMP 9/10 stimulation experiments were deemed necessary in order to assess that activated Smad4 represses Angpt-2, Apln, and Esm1. To determine which timepoint was best to BMP 9/10 stimulate the cells, I seeded another six-well plate with Nonsilencing (NS) shRNA MS1 cells, and exchanged to serum-free media after 36 hours. The next morning, I stimulated five wells at different times before protein collection: 4hrs, 2hrs, 1hr, 30min, and 0 min.
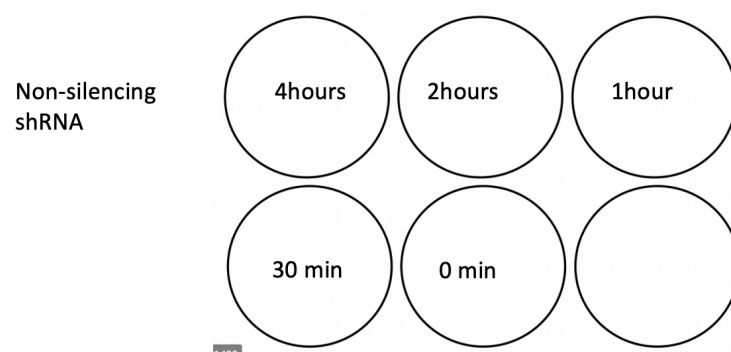
Figure 29 A schematic showing the experimental design of the BMP 9/10 stimulation test.

The Western blot below determined that BMP9/10 stimulation was best 4 hours before protein collection.
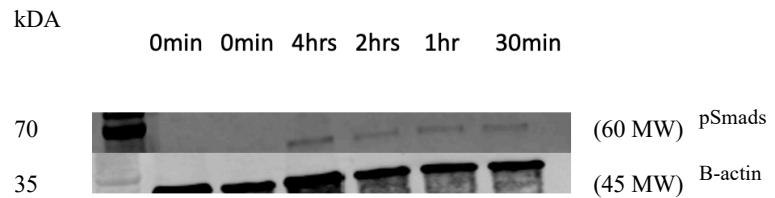
Figure 30 Western Blot showing the expression of phosphorylated Smads 1/4/5/9 at different timepoints of BMP 9/10 stimulation.

Now that the Smad4 knockdown level and BMP 9/10 stimulation was confirmed with protein, running a qPCR at the RNA level with Ang2, Apln, and ESM1 primers could confirm that Smad4 repression happens at the transcriptional level. I seeded NS shRNA MS1 cells into a six-well plate and Smad4KD shRNA MS1 cells into a six-well plate at a seeding density of 0.3x10^6 cells/well.
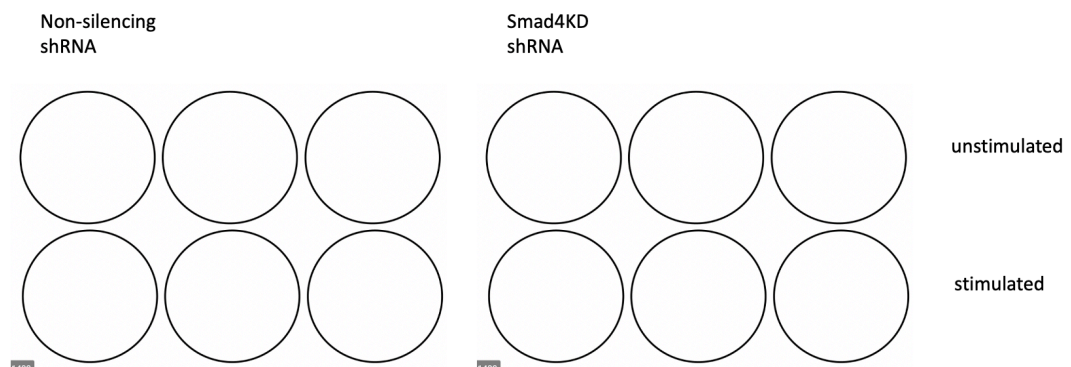
Figure 31 A schematic showing the experimental design of BMP 9/10 stimulated of two plates of MS1 cells, one with Nonsilencing shRNA, the other with Smad4 Knockdown shRNA.

After 36 hours, I placed the cells in serum-free media. The next morning, I stimulated three wells on each plate with BMP 9/10 four hours before I collected the RNA. The qPCR results are below.

30
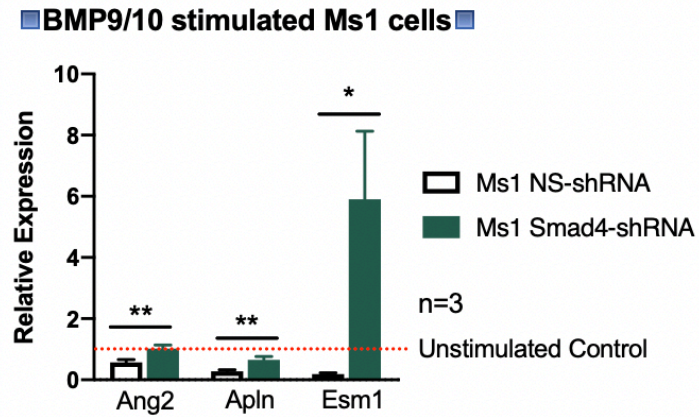
Figure 32 The qPCR results of the above experiment. The dotted red line shows the point of unstimulated control at 1, which is the reference point. In the Nonsilencing-shRNA samples, you can see repression of Ang2, Apln, and Esm1. In the Smad4-shRNA samples, you can see not as effective repression of Ang2 and Apln, and complete overexpression of Esm1.

As you can see, in the MS1 Smad4-shRNA samples, the relative expression of Ang2, Apln, and Esm1 are elevated compared to the control. However, the Smad4 KD level was not as robust as seen in previous experiments *in vivo* where the expression of Smad4 KD was much lower.
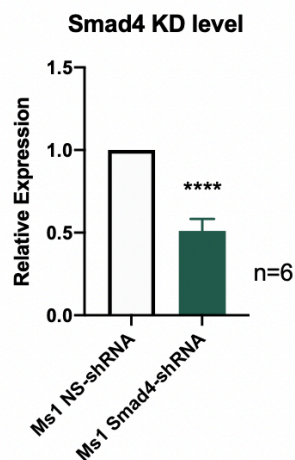
Figure 33 qPCR results showing the relative Smad4 KD level.

More repetitions of the experiment outlined above yielded similar results, wherein the Smad4 knockdown level was only reduced to approximately half of the NS-shRNA. Therefore, the qPCR results were not optimized with regards to Smad4's effect on Angpt-2, Apln, and Esm1. Because of this, a transition to using siRNA instead of shRNA to knock out Smad4 *in vitro* was pursued.

Smad4 siRNA Transfection Experiments

A transition to siRNA instead of shRNA was chosen since another person in the Meadows Lab showed a higher reduction in Smad4 in their qPCR experiments. Using a similar experimental design to the shRNA experiment, first, MS1 cells were seeded into a 6-well plate at a seeding density of 0.1x10^6 cells/well. After 24 hours, I transfected 3 wells with Nonsilencing siRNA and 3 with Smad4KD siRNA.

Nonsilencing siRNA

Smad4KD siRNA

Figure 34 A schematic showing the basic Nonsilencing and Smad4KD siRNA experimental design.

I collected protein the next day and ran a Western blot to ensure that Smad4 was knocked down and the transfection protocol was sufficient.
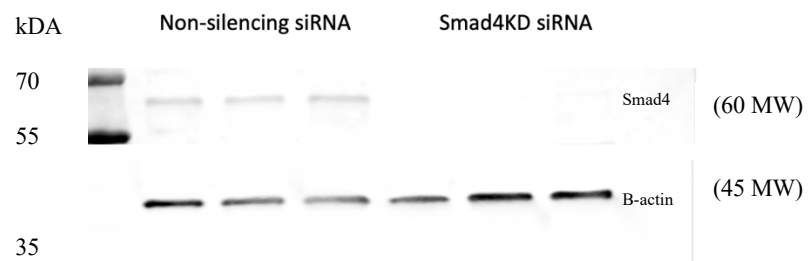
Figure 35 Western Blot showing the absence of Smad4 protein in the siRNA model.

Additionally, a confirmation of the best timepoint to stimulate the cells with BMP 9/10 was necessary since I was still working with MS1s, however these cells were not transfected with shRNA. I transfected one plate of MS1 cells with nonsilencing siRNA and placed the cells in serum-free media after 36 hours. The next morning, I stimulated the wells at different timepoints before protein collection: 4hrs, 2hrs, 1hr, 30min, and 0min.
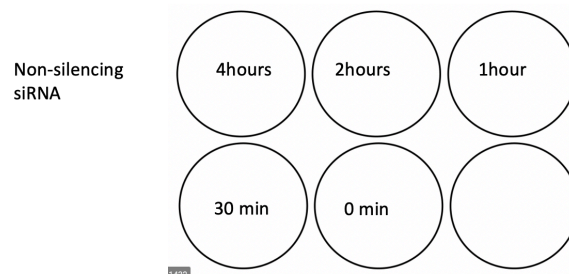
Figure 36 A schematic showing the experimental design of the BMP 9/10 stimulation test.

I collected the protein and ran the Western Blot below and determined that 1 hour was when phosphorylated Smads were most present.
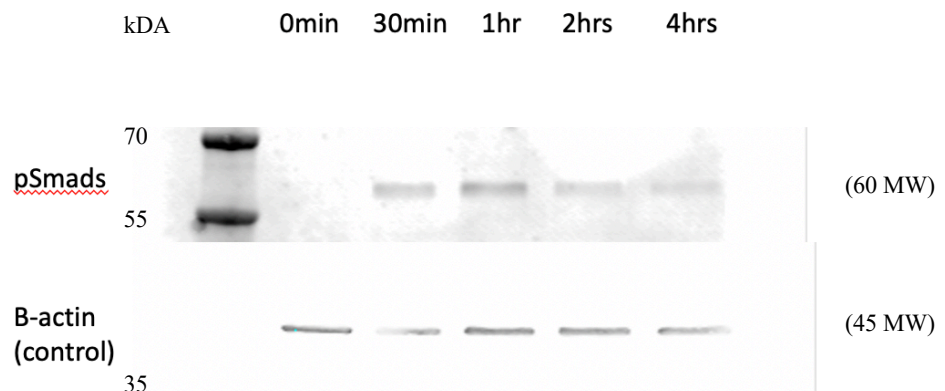
Figure 37 Western Blot showing the expression of phosphorylated Smads 1/4/5/9 at different timepoints of BMP 9/10 stimulation.

With that in mind, I set up an experiment to collect RNA. I seeded 2 six-well plates with MS1 cells at a seeding density of 0.1x10^6 cells/well. After 24 hours, I transfected one plate with nonsilencing siRNA and the other with Smad4 siRNA.
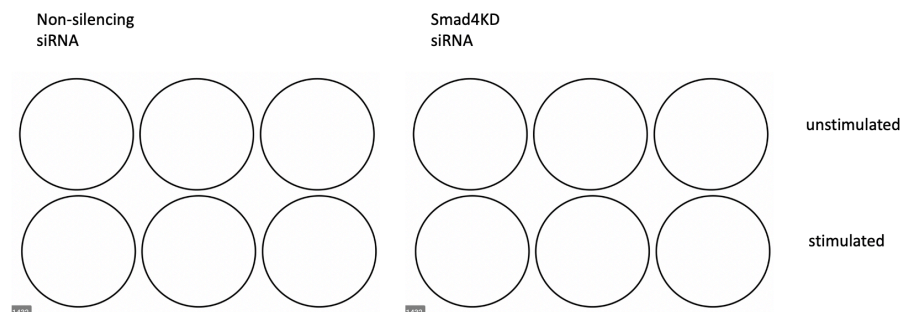

Figure 38 A schematic showing the experimental design of BMP 9/10 stimulated of two plates of MS1 cells, one with Nonsilencing siRNA, the other with Smad4 Knockdown siRNA.

After 36 hours, I placed the cells in serum-free media. The next morning, I stimulated three wells on each plate with BMP 9/10 1 hour before I collected the RNA.
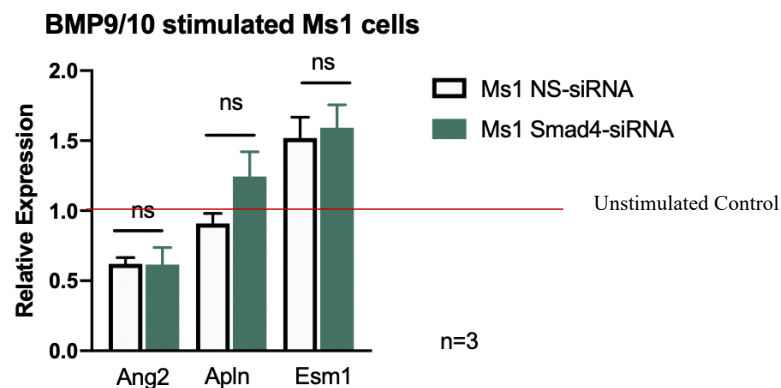
Figure 39 The qPCR results of the above experiment. The red line shows the point of unstimulated control at 1, which is the reference point. In the Nonsilencing-siRNA samples, Ang2 was not changed, while Apln and Esm1 were increased compared to previous results. Additionally, there was not a statistically difference between the NS and Smad4-siRNA treatments.

The qPCR results were different than the shRNA qPCR results, and we believed that this might be due to not enough time for phosphorylated Smad4 to repress effectors downstream in the control samples. But, the Smad4KD level was much more effective than in the shRNA experiments, as you can see below.
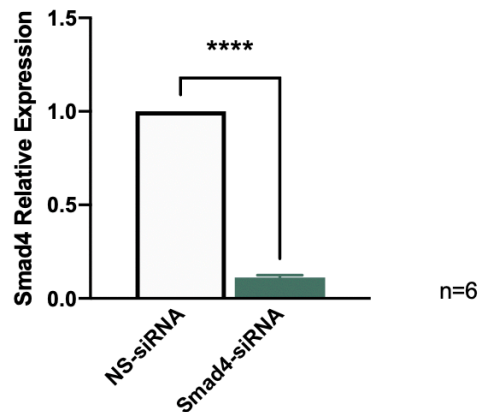
Figure 40 qPCR results showing the relative Smad4 KD level. Compared to **Figure 33**, you can see the knockdown level of Smad4 is much more effective (around 0.15 relative expression compared to 0.5).

I repeated the experiment, but this time stimulating two hours before RNA collection. However, the first time, the quality of the RNA was not sufficient for conclusive results. The last time, the experiments finally showed the expected results. As you can see below, the Smad4 KD level is dramatically reduced, around 0.1 relative expression. BMP 9/10 stimulation led to the repression of Ang2, Apln, and Esm1in Nonsilencing-siRNA samples, while Samd4-siRNA samples exhibited significant increases in expression of all three genes, with the Esm1 even being overexpressed above the unstimulated control.
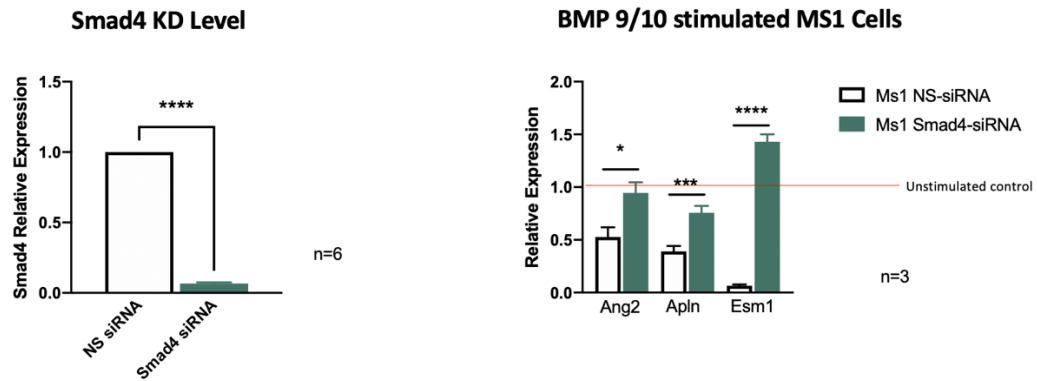
Figure 41 The final qPCR results. The Smad4 KD level is on the left, wherein the relative expression of Smad4 is down to 0.1. On the right, the qPCR results show the relative expression of Ang2, Apln, and Esm1 in Ms1 Smad4-siRNA compared to Ms1 NS-siRNA. The red line shows the point of unstimulated control at 1.0, which is the reference point. The repression of these three genes is statistically less in the Smad4-siRNA samples compared to the NS-siRNA samples, with Esm1 even being overexpressed.

Thus, the siRNA experiments were able to replicate the shRNA experiments and are more conclusive to show that Smad4 transcriptionally represses Ang2, Apln, and Esm1 *in vitro* since Smad4 is knocked down more effective. This experiment should be repeated again for confirmation.

Discussion

I believe it is important to secure conclusive *in vitro* results indicating whether Smad4 transcriptionally represses Angpt-2, Apln, and Esm1 or not. With more time, I would have repeated the siRNA experiments, since the Smad4 knock down level was very good compared to shRNA methods, to confirm that in the absence of Smad4, Angpt-2, Apln, and Esm1 are overexpressed.

Additionally, I would recommend using a Dual Luciferase Assay protocol to confirm binding of Smad4 to specific DNA points of control for Angpt-2, Apln, and Esm1. I tried using this protocol with MS1 cells and also 293T cells, which are easier to transfect. I also tried different seeding densities, different concentrations of DNA, and different positive controls to get a reading in the luminometer. No matter how I tried the protocol, the sample readings gave a "too low" error, so no data was ever collected. If given more time, getting this protocol to work will confirm more clearly that Smad4 binds to DNA regulatory regions to transcriptionally control for Angpt-2, Apln, and Esm1, strengthening the hypothesis that Smad4 is a direct transcriptional repressor of these genes and plays a role in regulating angiogenesis in HHT.

List of References

Augustin, Hellmut G et al. "Control of vascular morphogenesis and homeostasis through the angiopoietin-Tie system." *Nature reviews. Molecular cell biology* vol. 10,3 (2009): 165-77. doi:10.1038/nrm2639

Baeyens, Nicolas et al. "Defective fluid shear stress mechanotransduction mediates hereditary hemorrhagic telangiectasia." *The Journal of cell biology* vol. 214,7 (2016): 807-16. doi:10.1083/jcb.201603106

Barbara, N P et al. "Endoglin is an accessory protein that interacts with the signaling receptor complex of multiple members of the transforming growth factor-beta superfamily." *The Journal of biological chemistry* vol. 274,2 (1999): 584-94. doi:10.1074/jbc.274.2.584

Bari, Omar, and Philip R Cohen. "Hereditary hemorrhagic telangiectasia and pregnancy: potential adverse events and pregnancy outcomes." *International journal of women's health* vol. 9 373-378. 26 May. 2017, doi:10.2147/IJWH.S131585

Bayrak-Toydemir, Pinar et al. "A fourth locus for hereditary hemorrhagic telangiectasia maps to chromosome 7." *American journal of medical genetics. Part A* vol. 140,20 (2006): 2155-62. doi:10.1002/ajmg.a.31450

Bechard, D et al. "Characterization of the secreted form of endothelial-cell-specific molecule 1 by specific monoclonal antibodies." *Journal of vascular research* vol. 37,5 (2000): 417-25. doi:10.1159/000025758

Blanco, Francisco J et al. "Interaction and functional interplay between endoglin and ALK-1, two components of the endothelial transforming growth factor-beta receptor complex." *Journal of cellular physiology* vol. 204,2 (2005): 574-84. doi:10.1002/jcp.20311

Braverman, I M et al. "Ultrastructure and three-dimensional organization of the telangiectases of hereditary hemorrhagic telangiectasia." *The Journal of investigative dermatology* vol. 95,4 (1990): 422-7. doi:10.1111/1523-1747.ep12555569

Crist, Angela M et al. "Angiopoietin-2 Inhibition Rescues Arteriovenous Malformation in a Smad4 Hereditary Hemorrhagic Telangiectasia Mouse Model." *Circulation* vol. 139,17 (2019): 2049-2063. doi:10.1161/CIRCULATIONAHA.118.036952

Crist, Angela M et al. "Vascular deficiency of Smad4 causes arteriovenous malformations: a mouse model of Hereditary Hemorrhagic Telangiectasia." *Angiogenesis* vol. 21,2 (2018): 363-380. doi:10.1007/s10456-018-9602-0

Chapman, Nigel A et al. "The apelin receptor: physiology, pathology, cell signalling, and ligand modulation of a peptide-activated class A GPCR." *Biochemistry and cell biology = Biochimie et biologie cellulaire* vol. 92,6 (2014): 431-40. doi:10.1139/bcb-2014-0072

Derynck, Rik, and Ying E Zhang. "Smad-dependent and Smad-independent pathways in TGF-beta family signalling." *Nature* vol. 425,6958 (2003): 577-84. doi:10.1038/nature02006

Gallione, Carol et al. "Overlapping spectra of SMAD4 mutations in juvenile polyposis (JP) and JP-HHT syndrome." *American journal of medical genetics. Part A* vol. 152A,2 (2010): 333-9. doi:10.1002/ajmg.a.33206

Gómez, Martín Alonso, Ruiz, Oscar Fernando, & Otero, William. (2015). A Case Report of Hereditary Hemorrhagic Telangiectasia (HHT). *Revista Colombiana de Gastroenterologia*, *30*(4), 469-473. Retrieved November 01, 2020, from http://www.scielo.org.co/scielo.php?script=sci_arttext&pid=S0120-99572015000400011&lng=en&tlng=en.

Groppe, Jay et al. "Cooperative assembly of TGF-beta superfamily signaling complexes is mediated by two disparate mechanisms and distinct modes of receptor binding." *Molecular cell* vol. 29,2 (2008): 157-68. doi:10.1016/j.molcel.2007.11.039

Guttmacher, A E et al. "Hereditary hemorrhagic telangiectasia." *The New England journal of medicine* vol. 333,14 (1995): 918-24. doi:10.1056/NEJM199510053331407

Johnson, D W et al. "Mutations in the activin receptor-like kinase 1 gene in hereditary haemorrhagic telangiectasia type 2." *Nature genetics* vol. 13,2 (1996): 189-95. doi:10.1038/ng0696-189

Kasai, Atsushi et al. "Apelin is a novel angiogenic factor in retinal endothelial cells." *Biochemical and biophysical research communications* vol. 325,2 (2004): 395-400. doi:10.1016/j.bbrc.2004.10.042

Kjeldsen, A D et al. "Hereditary haemorrhagic telangiectasia: a population-based study of prevalence and mortality in Danish patients." *Journal of internal medicine* vol. 245,1 (1999): 31-9. doi:10.1046/j.1365-2796.1999.00398.

Lawton, Michael T et al. "Brain arteriovenous malformations." *Nature reviews. Disease primers* vol. 1 15008. 28 May. 2015, doi:10.1038/nrdp.2015.8

Livneh A et al. "Functionally reversible hepatic arteriovenous fistulas during pregnancy in patients with hereditary hemorrhagic telangiectasia." *Southern Medical Journal*. 1988 Aug;81(8):1047-1049. DOI: 10.1097/00007611-198808000-00026.

Mahmoud, Marwa et al. "Pathogenesis of arteriovenous malformations in the absence of endoglin." *Circulation research* vol. 106,8 (2010): 1425-33. doi:10.1161/CIRCRESAHA.109.211037

Masuyama, N., Hanafusa, H., Kusakabe, M., Shibuya, H. & Nishida, E. Identification of two Smad4 proteins in *Xenopus*. Their common and distinct properties. *J. Biol. Chem.* 274, 12163–12170 (1999)

McAllister, K A et al. "Endoglin, a TGF-beta binding protein of endothelial cells, is the gene for hereditary haemorrhagic telangiectasia type 1." *Nature genetics* vol. 8,4 (1994): 345-51. doi:10.1038/ng1294-345

Oh, S P et al. "Activin receptor-like kinase 1 modulates transforming growth factor-beta 1 signaling in the regulation of angiogenesis." *Proceedings of the National Academy of Sciences of the United States of America* vol. 97,6 (2000): 2626-31. doi:10.1073/pnas.97.6.2626

Owens, Christopher D. "Adaptive changes in autogenous vein grafts for arterial reconstruction: clinical implications." *Journal of vascular surgery* vol. 51,3 (2010): 736-46. doi:10.1016/j.jvs.2009.07.102

Plauchu, H et al. "Age-related clinical profile of hereditary hemorrhagic telangiectasia in an epidemiologically recruited population." *American journal of medical genetics* vol. 32,3 (1989): 291-7. doi:10.1002/ajmg.1320320302

Poduri, Aruna et al. "Endothelial cells respond to the direction of mechanical stimuli through SMAD signaling to regulate coronary artery size." *Development (Cambridge, England)* vol. 144,18 (2017): 3241-3252. doi:10.1242/dev.150904

Rochon, Elizabeth R et al. "Alk1 controls arterial endothelial cell migration in lumenized vessels." *Development (Cambridge, England)* vol. 143,14 (2016): 2593-602. doi:10.1242/dev.135392

Saito, Takako et al. "Structural Basis of the Human Endoglin-BMP9 Interaction: Insights into BMP Signaling and HHT1." *Cell reports* vol. 19,9 (2017): 1917-1928. doi:10.1016/j.celrep.2017.05.011

Thurston, Gavin, and Christopher Daly. "The complex role of angiopoietin-2 in the angiopoietin-tie signaling pathway." *Cold Spring Harbor perspectives in medicine* vol. 2,9 a006550. 1 Sep. 2012, doi:10.1101/cshperspect.a006650

Upton, Paul D et al. "Bone morphogenetic protein (BMP) and activin type II receptors balance BMP9 signals mediated by activin receptor-like kinase-1 in human pulmonary artery endothelial cells." *The Journal of biological chemistry* vol. 284,23 (2009): 15794-804. doi:10.1074/jbc.M109.002881